RSC Advances

PAPER

View Article Online
View Journal | View Issue

Cite this: *RSC Adv.*, 2017, **7**, 14224

Synthesis of SO_4^{2-}/TiO_2–$ZnAl_2O_4$ composite solid acids as the esterification catalysts

An-Qi Wang, Jun-Xia Wang,* Hui Wang, Ya-Nan Huang, Ming-Liang Xu and Xiu-Ling Wu*

Received 2nd February 2017
Accepted 13th February 2017

DOI: 10.1039/c7ra01386h

rsc.li/rsc-advances

A series of novel sulfated $ZnAl_2O_4$–TiO_2 ($SO_4^{2-}/ZnAl_2O_4$–TiO_2) composite solid acids were synthesized for the esterification of biomass derived acids. The properties were characterized by XRD, FT-IR, XPS, NH_3-TPD, acid–base titration, TG and FE-SEM. The experimental results showed that the introduction of $ZnAl_2O_4$ spinel oxide played a key role in stabilizing the structure of the composite catalysts as well as the surface sulfate groups. The composition of SO_4^{2-}/TiO_2–$ZnAl_2O_4$ catalysts significantly influenced their catalytic properties and performance in esterification reactions. The optimal $SO_4^{2-}/ZnAl_2O_4$–TiO_2 (6 : 4) catalyst with the largest number of acid sites showed superior conversion of 95.8% in oleic acid esterification and 98.5% conversion in acetic acid esterification. Moreover, the $SO_4^{2-}/ZnAl_2O_4$–TiO_2 (6 : 4) catalyst showed excellent reusability in these reactions, which was ascribed to its stable structure and good resistance of the surface sulfate groups. The efficient and reusable $SO_4^{2-}/ZnAl_2O_4$–TiO_2 composite solid acid coupled with spinel modification is expected to bring new opportunities in the design of favorable acid catalysts.

1. Introduction

Acid catalysts have wide applications in industrial reactions, such as esterification, alkylation, hydrogenation, *etc.*[1] Among them, the esterification of carboxylic acids with alcohols has attracted growing importance due to the continual demand for renewable fuels, pharmaceutical intermediates, solvents, coatings, *etc.*[1,2] In particular, esterification has gained much popularity in clean catalytic technologies for the conversion of biomass-derived chemicals into biofuels production.[2] It was generally catalyzed by mineral acids because of their high activities and low prices. However, mineral acids accelerate the corrosion of equipment, and the residual acids are difficult to remove from the product stream. As a green alternative of the mineral acid, solid acid catalysts have important advantages of being non-corrosive, easy separation procedures, good reusability, *etc.*[3]

Currently, a number of solid acids have been investigated in esterification, such as cation-exchange resins, clays, sulfated metal oxide (SO_4^{2-}/M_xO_y), activated carbons, zeolites, MOFs.[4–6] The SO_4^{2-}/TiO_2 catalyst, a representative SO_4^{2-}/M_xO_y solid acid, is used extensively in esterification because of its outstanding performance of high catalytic activity, good selectivity, easy separation and so on.[7] However, pure SO_4^{2-}/TiO_2 catalysts usually suffer from rapid deactivation and low life despite their high initial activities, which is mainly due to the loss of sulfur species and carbon deposition.[8,9] Therefore, development of acid catalysts for liquid reaction is still a challenge from the view of not only high activity but also stability and life. To date, several M_xO_y oxides, including ZrO_2, Al_2O_3, Fe_3O_4, *etc.* have been studied widely in the synthesis of SO_4^{2-}/TiO_2–M_xO_y composite solid acids because of the apparent improvement in catalytic activities and reusability.[8–11] In our previous study, the $ZnAl_2O_4$ spinel-type oxide was used successfully to obtain the sulfated $ZnAl_2O_4$ solid acid which has the advantage of easy preparation, single crystal shape, stable structure and good performance in acetic esterification.[12–14] It is therefore expected that using the $ZnAl_2O_4$ spinel-type oxide as M_xO_y to synthesize the SO_4^{2-}/TiO_2–M_xO_y composite may result in interesting properties and catalytic activities. In addition, it is generally accepted that metal oxides (M_xO_y) have their own superior catalytic crystallographic form.[15,16] For example, titania was reported to have three crystallographic forms, including anatase, rutile and brookite. Among them, the anatase form of titania was regard as the most active form.[15] Similarly, it was reported that spinel was the favorable form to perform catalytic activities in reactions for sulfated $ZnAl_2O_4$ oxides.[12] Hence, it is necessary to maintain the superior crystallographic forms of TiO_2 and $ZnAl_2O_4$ in the composite catalysts in this study.

To develop a catalyst with superior acid properties and stability, SO_4^{2-}/TiO_2–$ZnAl_2O_4$ solid acids were synthesized by compositing TiO_2 and $ZnAl_2O_4$ oxides. The main aim was to maintain both the catalytic crystallographic forms of respective TiO_2 and $ZnAl_2O_4$ components, which was a unique advantage compared to other SO_4^{2-}/TiO_2–M_xO_y composite solid acids. Moreover, this study modulated the acidic properties of SO_4^{2-}/TiO_2–$ZnAl_2O_4$ catalysts by adjusting the mass ratio of TiO_2/

Faculty of Materials Science and Chemistry, Engineering Research Center of Nano-Geomaterials of Ministry of Education, China University of Geosciences, Wuhan 430074, China. E-mail: wjx76@sina.com; xlwu@cug.edu.cn

$ZnAl_2O_4$ components. The obtained acid catalysts with different compositions were evaluated in the liquid-phase esterification of acetic acid with acetic acid with *n*-butanol and oleic acid with methanol. The esterification of oleic acid with methanol has attracted great interest in biodiesel production, as the oleic acid is a common type of free fatty acids (FFAs) existing in plant oils.[17,18] The esterification of acetic acid, as a representative acid in initial bio-oils, can efficiently improve the stability and heating value of bio-oils.[19,20] The product from the esterification of acetic acid with *n*-butanol is a common green chemical. In addition, it also discussed the roles of respective components present in the $SO_4^{2-}/ZnAl_2O_4$–TiO_2 composite catalyst. In the meantime, we assumed the relationships between catalyst composition, catalytic performances structure and acidic properties. To date, there are few studies on $SO_4^{2-}/ZnAl_2O_4$–TiO_2 solid acid catalysts, which are regarded as a referential study for the modification of SO_4^{2-}/M_xO_y solid acid catalyst.

2. Experimental

2.1 Catalysts preparation

The $ZnAl_2O_4$–TiO_2 was synthesized by a two-step sol–gel method. $ZnAl_2O_4$ powders were prepared according to the procedure of the sol–gel method mentioned in a former study.[12] The $Al(NO_3)_3\cdot 9H_2O$ and $Zn(NO_3)_2\cdot 6H_2O$ with a molar ratio of 2 : 1 were dissolved in ethanol with magnetic stirring. Moreover, 5 wt% (based on total mass of metal nitrate) of polyethylene glycol was added to the mixture solution with magnetic stirring for 4 h at room temperature. The solution was evaporated with further stirring for 2 h in a water bath at 60 °C to obtain the sol. The sol was dried and ground. The obtained powder was calcined at 600 °C for 5 h in air to obtain the spinel $ZnAl_2O_4$. The Ti-contained sol–gel hydrolysis was formed by adding $Ti(OC_4H_9)_4$ (titanium butoxide) dropwise into a mixture solution, which contained water, ethanol and acetic acid. The volume ratio of the titanium butoxide, water, ethanol and acetic acid in the mixed solution was 1 : 0.76 : 1 : 1. Thereafter, a calculated amount of $ZnAl_2O_4$ powder was added to the mixed solution to stir for 4 h and then evaporated with stirring for 1 h in a water bath at 65 °C. The obtained sol was dried overnight at 100 °C and ground into fine powders. The obtained powders were sulfated by impregnating with a 0.75 mol L^{-1} $(NH_4)_2SO_4$ solution for 4 h. Subsequently, it was dried at 80 °C for 4 h and ground. The resulting powders were calcined at 500 °C for 3 h in air to obtain the $SO_4^{2-}/ZnAl_2O_4$–TiO_2 catalysts. The $SO_4^{2-}/ZnAl_2O_4$–TiO_2 catalysts with different mass ratios of $ZnAl_2O_4$ to TiO_2, including 1 : 0, 8 : 2, 6 : 4, 4 : 6, 2 : 8 and 0 : 1, were denoted as $SO_4^{2-}/ZnAl_2O_4$, $SO_4^{2-}/ZnAl_2O_4$–TiO_2 (8 : 2), $SO_4^{2-}/ZnAl_2O_4$–TiO_2 (6 : 4), $SO_4^{2-}/ZnAl_2O_4$–TiO_2 (4 : 6), $SO_4^{2-}/ZnAl_2O_4$–TiO_2 (2 : 8) and SO_4^{2-}/TiO_2, respectively. The reused mixed oxide catalysts after three repeated cycles were denoted as $SO_4^{2-}/ZnAl_2O_4$-used, $SO_4^{2-}/ZnAl_2O_4$–TiO_2 (6 : 4)-used, and SO_4^{2-}/TiO_2-used.

2.2 Catalysts characterization

Wide angle X-ray diffraction (XRD) was conducted on a Bruker AXS D8-Focus X Diffractometer using CuKα radiation at 40 kV and 40 mA. The data were collected by varying the 2θ from 10° to 70°; the Fourier transform infrared spectroscopy (FT-IR) spectra of the catalysts were recorded in the range of 400–4000 cm^{-1} by a Nicolet 6700 IR spectrometer, and the catalyst was pretreated by drying for 4 h at 60 °C and subjected to KBr pellet technique. The morphology of the catalysts was examined by Field Emission Scanning Electron Microscopy (FE-SEM) on a SU 8010 electron microscope. The dried samples were coated with a thin film of gold. X-ray Photoelectron Spectroscopy (XPS) was performed on a VG Multilab 2000. A NH_3 Temperature Programmed Desorption (NH_3-TPD) experiment was carried out using a Micromeritics AutoChem II 2920 quipped with a TCD detector and the sample was heated from room temperature to 400 °C at a rate of 10 °C min^{-1} and further treated in a helium flow (50 mL min^{-1}). The samples were then exposed to NH_3 (50 mL min^{-1}) at room temperature for 1 h, followed by helium to remove the gas-phase and physically adsorbed NH_3. Measurements were carried out in helium at a heating rate of 10 °C min^{-1}. Thermogravimetric analysis (TG) was performed on a STA449F3 thermo analyzer from room temperature to 800 °C with a ramp rate of 10 °C min under 30 mL min^{-1} flow of a nitrogen oxygen mixture. The acid site density of the catalysts was determined using ion-exchange titration. Moreover, 200 mg of the catalyst was added to 50 mL of a 0.1 mol L^{-1} NaCl solution and stirred for 24 h at room temperature. The catalyst was separated by filtration. The filtrate with two drops of a phenolphthalein solution was titrated against 0.01 mol L^{-1} NaOH solution to neutrality. The total acid densities of the catalysts were estimated by calculating the amount of NaOH consumed.[21,22]

2.3 Catalytic activity test

The esterification of acetic acid with *n*-butanol was carried out in a three-necked flask equipped with a magnetic stirrer, a thermometer and a reflux condenser tube. A 1 : 3 molar ratio of acetic acid to *n*-butanol and 7.26 wt% catalyst, based on the weight of acetic acid, were added to a three-necked flask. The reaction was carried out under the atmospheric pressure, and the temperature was controlled in the range of 112–115 °C for 2 h. The formed water was removed continuously by becoming an azeotrope with *n*-butanol to drive the equilibria to completion.

The esterification of oleic acid with methanol was carried out in 50 mL autoclave immersed in an oil bath. The reactors were initially loaded with the reaction mixture consisting of a 5 wt% (based on the oleic acid) of catalysts and a 1 : 10 molar ratio of oleic acid and methanol. The autoclave was sealed and immersed in the oil bath at 100 °C for 2 h.

The conversion of acids can be calculated by titration according to the report of Pires *et al.*[23] and the method of GB1668-81 using the following equation:

$$\text{Conversion of acid } (\%) = \frac{M_0 - M_1}{M_0} \times 100$$

where M_0 is the acid value before the reaction and M_1 is the acid value after the reaction. 0.50 mL initial or final reaction mixture

was added to 20.00 mL ethanol and titrated by 0.10 mol L^{-1} NaOH solution using phenolphthalein as an indicator. The acid base titration was also performed with time to estimate the conversion of acid based on the acid value.

The used $SO_4^{2-}/ZnAl_2O_4$, $SO_4^{2-}/ZnAl_2O_4$–TiO_2 (6 : 4) and SO_4^{2-}/TiO_2 catalysts were recovered by filtering and drying, after completing each reaction.

3. Results and discussion

3.1 Characterization of the catalysts

Fig. 1 shows the XRD patterns of $SO_4^{2-}/ZnAl_2O_4$, SO_4^{2-}/TiO_2 and $SO_4^{2-}/ZnAl_2O_4$–TiO_2 catalysts. The characteristic diffraction peaks of $ZnAl_2O_4$ spinel (JCPDS no. 05-0669) at 2θ values of 31.3°, 36.9°, 44.9°, 49.1°, 55.7°, 59.4° and 65.3° were present in the $SO_4^{2-}/ZnAl_2O_4$ and $SO_4^{2-}/ZnAl_2O_4$–TiO_2 catalysts. The other peaks, located at 25.3°, 37.8°, 48.1°, 54.6° and 62.8°, were all assigned to the anatase phase (JCPDS no. 65-5714), which could be observed in SO_4^{2-}/TiO_2 and $SO_4^{2-}/ZnAl_2O_4$–TiO_2. The diffraction intensity for the respective phases was changed by varying the mass ratio of the two components. Moreover, there was no detectable impurity. This indicated that $SO_4^{2-}/ZnAl_2O_4$–TiO_2 catalysts only contained the simple spinel phase and anatase phase which were the catalytic crystallographic forms of the two component oxides.

The surface sulfate groups are responsible for inducing acidity in the catalyst. It has been assumed that the sulfate group is bonded covalently to the oxide.[24] All the catalysts shown in Fig. 2 exhibited a broad peak between 900 and 1400 cm^{-1}, which was assigned to sulfate groups bonded covalently to the surface metal oxides (Scheme 1a and b).[25,26] The sulfate group belonged to C_{2v} symmetry can be bonded to surface metals by two oxygen atoms forming bridge (Scheme 1a) or chelate structures (Scheme 1b). The broad peaks of all catalysts could be divided into three peaks at 1227, 1139 and 1060 cm^{-1}. Peaks at 1139 and 1060 cm^{-1} were ascribed to asymmetric and symmetric stretching of S–O bonds, respectively, and the others at 1398 and 1227 cm^{-1} were due to asymmetric and symmetric

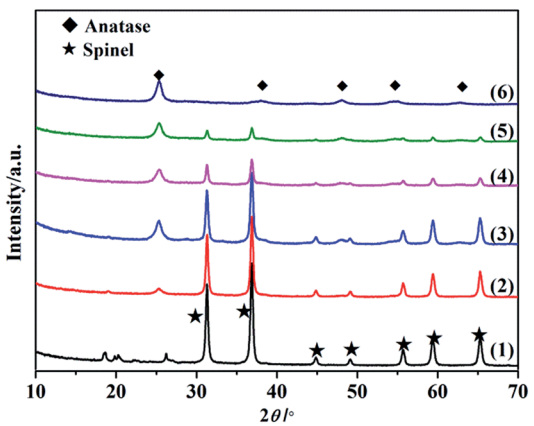

Fig. 1 XRD patterns of (1) $SO_4^{2-}/ZnAl_2O_4$, (2) $SO_4^{2-}/ZnAl_2O_4$–TiO_2 (8 : 2), (3) $SO_4^{2-}/ZnAl_2O_4$–TiO_2 (6 : 4), (4) $SO_4^{2-}/ZnAl_2O_4$–TiO_2 (4 : 6), (5) $SO_4^{2-}/ZnAl_2O_4$–TiO_2 (2 : 8) and (6) SO_4^{2-}/TiO_2 catalysts.

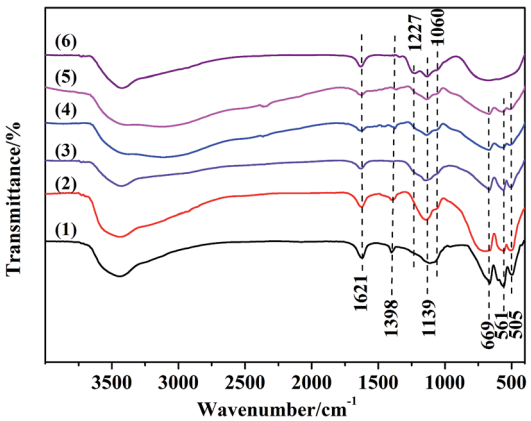

Fig. 2 FT-IR spectra of (1) $SO_4^{2-}/ZnAl_2O_4$, (2) $SO_4^{2-}/ZnAl_2O_4$–TiO_2 (8 : 2), (3) $SO_4^{2-}/ZnAl_2O_4$–TiO_2 (6 : 4), (4) $SO_4^{2-}/ZnAl_2O_4$–TiO_2 (4 : 6), (5) $SO_4^{2-}/ZnAl_2O_4$–TiO_2 (2 : 8) and (6) SO_4^{2-}/TiO_2 catalysts.

stretching of the S=O.[26,27] The peaks at 1227 cm^{-1} indicated that bonded sulfate groups were formed with the chelate structure (Scheme 1b).[28] In addition, the peaks that belonged to Al–O, Zn–O and Al–O vibrations for $ZnAl_2O_4$ spinel were observed at 669, 561 and 505 cm^{-1} in all $SO_4^{2-}/ZnAl_2O_4$–TiO_2 catalysts.[29] The existence of a spinel phase in mixed oxides catalysts was consistent with the results of XRD. The broad band in the range of 400–800 cm^{-1} occurred in SO_4^{2-}/TiO_2 was regarded as the stretching vibration of Ti–O–Ti. The broad band was not detected clearly in $SO_4^{2-}/ZnAl_2O_4$–TiO_2, which might be due the band being covered by the intense peaks of Zn–O and Al–O vibrations.[30] In addition, peaks at 1621 and 3400 cm^{-1} were associated with the bending mode and stretching mode of the OH group of water molecules, respectively.[27]

In the XPS spectra for the $SO_4^{2-}/ZnAl_2O_4$–TiO_2 (6 : 4), the peaks for Zn 2p, Al 2p, Ti 2p, O 1s and S 2p were presented in Fig. 3. The spectra centered at 169.4 eV, corresponding to S 2p binding energy, was typical of the S^{6+} high oxidation state. This high oxidation state is essential evidence of formation of bidentate sulfate group, indicating that catalyst possessed acid sites.[30] In addition, the O 1s spectra in Fig. 3c can be decomposed into three peaks at 530.4 eV, 531.4 eV and 532.3 eV, which were assigned to lattice oxygen of metal oxide, bridged oxygen of surface hydroxyl groups and the oxygen of sulfate group, respectively.[31] For the oxidation state of the metal elements, the peaks at 1045.8 eV and 1022.7 eV shown in Fig. 3d belonged to Zn $2p_{1/2}$ and Zn $2p_{3/2}$ of Zn^{2+} ion.[32] Fig. 3e shows the Al 2p peak of the catalyst at 75.2 eV, which was assigned to the Al^{3+} ion.[33] The binding energy of Ti $2p_{3/2}$, shown in Fig. 3f, was 459.1 eV

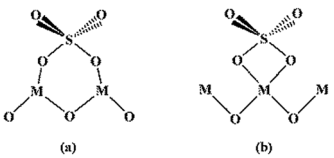

Scheme 1 Structure of bonded sulfate group with C_{2v} bridge (a) and bonded sulfate ion with C_{2v} chelate (b).

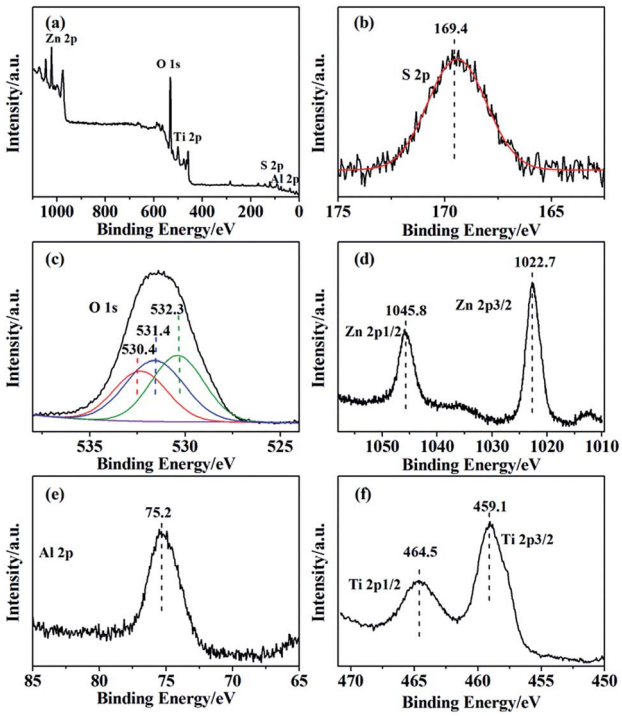

Fig. 3 XPS spectra of the (a) $SO_4^{2-}/ZnAl_2O_4$–TiO_2 (6 : 4) catalysts and the high-resolution photoelectron spectra of (b) Zn 2p, (c) Al 2p, (d) S 2p, (e) O 1s and (f) Ti 2p.

and that of Ti $2p_{1/2}$ was 464.5 eV, revealing that Ti was in the 4+ oxidation state.[34]

NH_3-TPD was used to estimate the amount and strength of acid sites formed on the surface of the catalysts. All the $SO_4^{2-}/ZnAl_2O_4$, $SO_4^{2-}/ZnAl_2O_4$–TiO_2 and SO_4^{2-}/TiO_2 catalysts contain a certain amount of acid sites, indicating both TiO_2 and $ZnAl_2O_4$ acted as active components to form the acid sites on the surface by sulfation. The broadened peaks, shown in Fig. 4, were divided into peaks assigned to weak acid sites (below 200 °C), middle strength acid sites (200–400 °C) and strong acid sites (above 400 °C).[35] These profiles showed that the catalysts contained various amounts of acid sites and different acid strengths. Compared to $SO_4^{2-}/ZnAl_2O_4$ and SO_4^{2-}/TiO_2, the $SO_4^{2-}/ZnAl_2O_4$–TiO_2 contained the largest number of acid sites with a clear increase in weak and middle strength acid sites. This may be explained that the synergistic interaction of two active components improved the generation of acid sites, which was commonly observed in the modified SO_4^{2-}/TiO_2–M_xO_y composite catalysts.[35,36] Moreover, the acid site density of the catalysts with different compositions was studied by the acid–base titration, as shown in Table 2. The mass ratio of $ZnAl_2O_4$ and TiO_2 had a strong effect on the acid site density of the catalysts. With increasing TiO_2 component, the acid site density was improved gradually. $SO_4^{2-}/ZnAl_2O_4$–TiO_2 (6 : 4) showed a higher density of acid sites than $SO_4^{2-}/ZnAl_2O_4$ and SO_4^{2-}/TiO_2, which is in agreement with NH_3-TPD. However, excess TiO_2 had a negative influence in acid site density. This may be due to the accumulation of TiO_2 on the outer surface of $ZnAl_2O_4$, which can be seen in other composite catalysts.[37] It was suggested that the acidic properties of $SO_4^{2-}/ZnAl_2O_4$–TiO_2 can be tuned by the mass ratio of the $ZnAl_2O_4$ and TiO_2 components and the acidic property was maximized with the optimal ratio of 6 : 4.

TG analysis of the $SO_4^{2-}/ZnAl_2O_4$, $SO_4^{2-}/ZnAl_2O_4$–TiO_2 (6 : 4) and SO_4^{2-}/TiO_2 catalysts was carried out, as shown in Fig. 5. The initial weight loss (around 100–200 °C) on the TG profiles was assigned to the desorption of physically adsorbed water.[37] Further increasing the temperature from 200 °C to 550 °C led to a gradual weight loss due to the removal of surface hydroxyl groups.[38] The third weight loss that started at about 550 °C was associated with the decomposition of surface sulfate groups, which was a typical feature in the TG profiles of SO_4^{2-}/M_xO_y.[38] Based on the TG profiles, the weight percentages of the sulfate groups eliminated from $SO_4^{2-}/ZnAl_2O_4$, $SO_4^{2-}/ZnAl_2O_4$–TiO_2 (6 : 4) and SO_4^{2-}/TiO_2 were estimated to be 13.1%, 20.2% and 16.5%, respectively, as shown in Table 1. This also proved that both TiO_2 and $ZnAl_2O_4$ acted as active components to generate surface sulfate groups after sulfation. Moreover, more the weight losses, more the sulfate groups that exist.[13,38] Thus, it was revealed that the $SO_4^{2-}/ZnAl_2O_4$–TiO_2 (6 : 4) catalyst contained more sulfate groups over their pure components, which may be due to the cooperation of $ZnAl_2O_4$ and TiO_2. This result was consistent with that of NH_3-

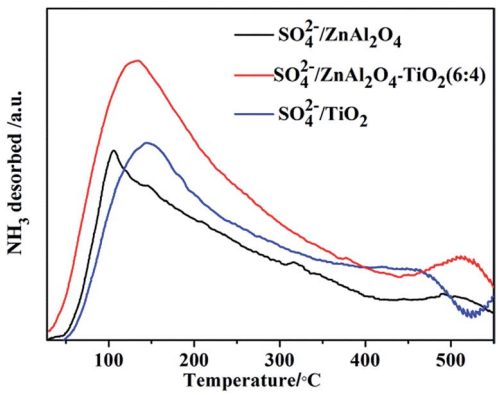

Fig. 4 NH_3-TPD profiles of $SO_4^{2-}/ZnAl_2O_4$, $SO_4^{2-}/ZnAl_2O_4$–TiO_2 (6 : 4) and SO_4^{2-}/TiO_2 catalysts.

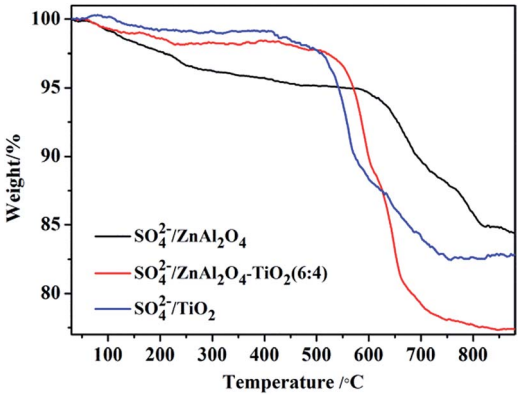

Fig. 5 TG curves of $SO_4^{2-}/ZnAl_2O_4$, $SO_4^{2-}/ZnAl_2O_4$–TiO_2 (6 : 4) and SO_4^{2-}/TiO_2 catalysts.

Table 1 Weight percentages of the sulfate groups based on the TG analysis

	Sulfate groups content[a] (%)		
Run number	SO_4^{2-}/$ZnAl_2O_4$	SO_4^{2-}/$ZnAl_2O_4$–TiO_2 (6 : 4)	SO_4^{2-}/TiO_2
1 (fresh)	13.1	20.2	16.5
3	10.9	16.2	7.8

[a] Based on the TG profiles from 550 °C to 800 °C.

TPD. In addition, the decomposition temperatures of sulfate groups were 660, 610 and 550 °C for SO_4^{2-}/$ZnAl_2O_4$, SO_4^{2-}/$ZnAl_2O_4$–TiO_2 (6 : 4) and SO_4^{2-}/TiO_2 respectively, indicating that the sulfate groups on $ZnAl_2O_4$-based catalysts showed better thermal stability than that of SO_4^{2-}/TiO_2 catalysts. This suggests that the $ZnAl_2O_4$ component might help stabilize surface sulfate groups by enhancing its thermal stability.

Fig. 6 shows FE-SEM images of SO_4^{2-}/$ZnAl_2O_4$, SO_4^{2-}/$ZnAl_2O_4$–TiO_2 and SO_4^{2-}/TiO_2 catalysts. The SO_4^{2-}/$ZnAl_2O_4$ catalyst, shown in Fig. 6a, had a near spherical particle appearance. However, Fig. 6b revealed plate-like morphologies of pure SO_4^{2-}/TiO_2. As shown in Fig. 6c, the morphology of SO_4^{2-}/$ZnAl_2O_4$–TiO_2 (6 : 4) showed that both $ZnAl_2O_4$ and TiO_2 kept up their unique morphologies. Moreover, spherical $ZnAl_2O_4$ particles were dispersed on or crossed through plate-like TiO_2 bulk. This further confirmed that the two components were composited in SO_4^{2-}/$ZnAl_2O_4$–TiO_2 (6 : 4) catalyst.

On the basis of the abovementioned characterization, the possible structures are shown in Fig. 7. The XPS corroborating FT-IR analysis gave the possible chelate structure of sulfate groups bonded on the surface metal oxides of catalysts. FE-SEM showed that spherical $ZnAl_2O_4$ particles were dispersed on or crossed through plate-like TiO_2 particles, and the M–O–Ti linkages were expected on the interface, resulting from the cooperation of two components, which may have improved the acidic properties of the composite catalysts.

3.2 Catalytic performance

The esterification of acetic acid with *n*-butanol and oleic acid with methanol (Scheme 2) were conducted over SO_4^{2-}/$ZnAl_2O_4$, SO_4^{2-}/TiO_2 and SO_4^{2-}/$ZnAl_2O_4$–TiO_2 catalysts. The effects of the different mass ratios of $ZnAl_2O_4$ to TiO_2 on the catalytic activities of SO_4^{2-}/$ZnAl_2O_4$–TiO_2 are shown in Fig. 8. Increasing the mass ratio of TiO_2 could significantly enhance the catalytic

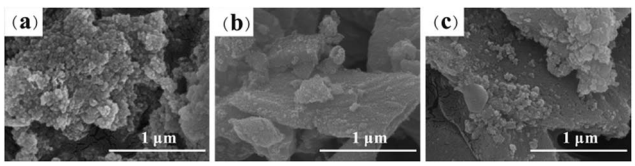

Fig. 6 FE-SEM micrographs of (a)SO_4^{2-}/$ZnAl_2O_4$, (b) SO_4^{2-}/TiO_2 and (c) SO_4^{2-}/$ZnAl_2O_4$–TiO_2 (6 : 4) catalysts.

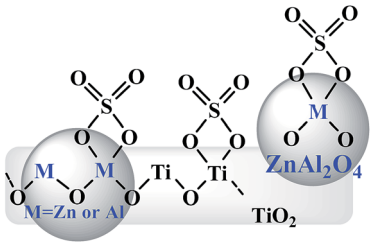

Fig. 7 Possible structures of the sulfate groups formed on the surface of SO_4^{2-}/$ZnAl_2O_4$–TiO_2 catalysts.

$$CH_3COOH + C_4H_9OH \overset{H^+}{\rightleftharpoons} CH_3COOC_4H_9 + H_2O \quad (1)$$

$$C_{17}H_{33}COOH + CH_3OH \overset{H^+}{\rightleftharpoons} C_{17}H_{33}COOCH_3 + H_2O \quad (2)$$

Scheme 2 Esterification of (1) acetic acid with *n*-butanol and (2) oleic acid with methanol.

activities of the SO_4^{2-}/$ZnAl_2O_4$–TiO_2 catalysts for both reactions. When the mass ratio of $ZnAl_2O_4$ to TiO_2 was 6 : 4, the catalytic activities were maximized for both reactions, with

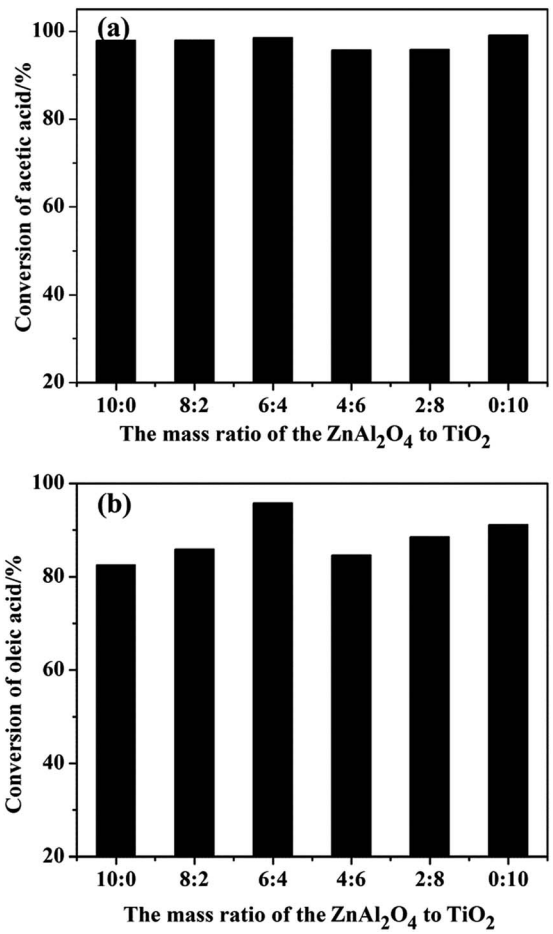

Fig. 8 Esterification of (a) acetic acid with *n*-butanol and (b) oleic acid with methanol over varied catalysts.

98.5% conversion for the esterification of acetic acid with *n*-butanol and 95.8% conversion for oleic acid esterification. The improvement in catalyst activities may be due to the increase in the number of acid sites, which had been characterized in the NH_3-TPD, acid–base titration and TG analysis. By further increasing the mass ratio of the TiO_2 component, the conversion of composite catalysts decreased, which was attributed to the reduction of the number of acid sites. The composition of catalyst clearly influenced the catalytic activities of the SO_4^{2-}/TiO_2–$ZnAl_2O_4$ composite in these reactions by adjusting their acidic properties. Furthermore, the reactivity of the active sites was investigated in terms of the turnover frequency (TOF), shown in Table 2. The results similarly demonstrated that the active sites present on SO_4^{2-}/$ZnAl_2O_4$–TiO_2 (6 : 4) showed a comparable rate per active site to that of SO_4^{2-}/TiO_2 and much greater efficiency than that of SO_4^{2-}/$ZnAl_2O_4$. This indicates that both $ZnAl_2O_4$ and TiO_2 can produce active sites to catalyze the esterification after sulfation. Moreover, the TiO_2 component acted as the main catalytic promotor in the composite to generate superior acid sites. The obtained SO_4^{2-}/$ZnAl_2O_4$–TiO_2 (6 : 4) was suggested to be an efficient catalyst for these two types of esterifications.

It is generally accepted that different esterification reactions have their preferential acid sites in terms of acidic strength.[39,40] In this study, the amounts of acid sites with different acidic strengths were calculated based on the NH_3-TPD profiles. Fig. 9 shows that the SO_4^{2-}/$ZnAl_2O_4$–TiO_2 (6 : 4) catalyst showed different acidic properties from SO_4^{2-}/$ZnAl_2O_4$ and SO_4^{2-}/TiO_2 catalysts, which may indicate their different catalytic activities. It was found that the trend of acetic acid conversion corresponded to the number of strong acid sites. On the other hand, the change in catalytic activities in oleic acid esterification increased in line with middle strength acid sites or weak acid sites. These two reactions may have their own favorable acid strength of acid sites. The relationship between acidic properties and catalytic activities gave a referential study for the design of catalysts for these reactions.

In order to develop a green and reusable catalyst, the capability of the catalyst to be recovered and reused should be considered seriously in the study of SO_4^{2-}/M_xO_y solid acids. Thus, SO_4^{2-}/$ZnAl_2O_4$, SO_4^{2-}/TiO_2 and optimal SO_4^{2-}/$ZnAl_2O_4$–TiO_2 (6 : 4) solid acid catalysts were recycled to study the

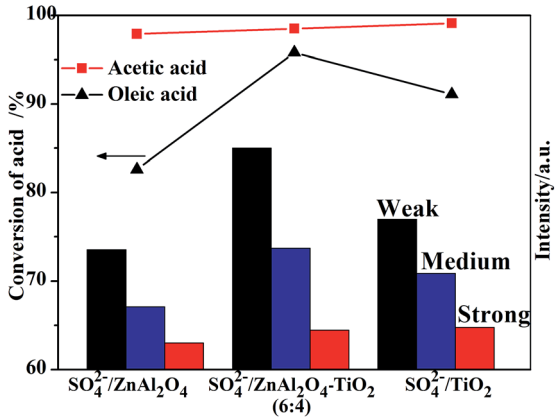

Fig. 9 Conversion of different acids and intensity of acidic amount as a function of SO_4^{2-}/$ZnAl_2O_4$, SO_4^{2-}/TiO_2 and SO_4^{2-}/$ZnAl_2O_4$–TiO_2 (6 : 4) catalysts with different acidic strengths.

stability of catalytic activity. As shown in Fig. 10, spinel-based catalysts outperformed SO_4^{2-}/TiO_2 catalyst in terms of the reusability for both reactions. This advantage was evidently manifested in the SO_4^{2-}/$ZnAl_2O_4$–TiO_2 (6 : 4) catalysts. Fig. 10a shows that SO_4^{2-}/$ZnAl_2O_4$–TiO_2 (6 : 4) can maintain the conversion of acetic acid above 85% in the fifth cycle, while SO_4^{2-}/TiO_2 showed a clear deactivation (~80%) after two repeated cycles. The catalytic activities for the esterification of oleic acid with methanol was ~40% and ~8% lower in reused SO_4^{2-}/TiO_2 and SO_4^{2-}/$ZnAl_2O_4$–TiO_2 (6 : 4), respectively, in the second cycle (Fig. 10b). These results show that the SO_4^{2-}/$ZnAl_2O_4$–TiO_2 (6 : 4) catalyst as a reusable catalyst can be recycled several times.

To study the stability and the reason for the deactivation, the used catalysts after two repeated cycles were characterized by XRD, FT-IR and TG, as shown in Fig. 11. According to FT-IR and XRD analysis, no evident change in the structure of the used SO_4^{2-}/$ZnAl_2O_4$–TiO_2 (6 : 4) catalyst was observed by comparing to the fresh catalyst. This indicated that SO_4^{2-}/$ZnAl_2O_4$–TiO_2 (6 : 4) had good structural stability after recycling. The IR spectra, shown in Fig. 11b, also gave broadened peaks of surface sulfate group in the range of 900–1400 cm^{-1}. The peaks of sulfate groups almost disappeared in the IR spectra of used SO_4^{2-}/TiO_2, while they were kept relatively better in the spectra

Table 2 Catalytic activities of sulfated catalysts for the catalysis of the acetic acid and oleic acid esterification

		Conv. (%)		TOF[a] (min^{-1})	
Catalysts	Acid sites (mmol g^{-1})	Acetic acid (20 min)	Oleic acid (30 min)	Acetic acid	Oleic acid
SO_4^{2-}/$ZnAl_2O_4$	1.84	45.3	50.2	2.81	0.57
SO_4^{2-}/$ZnAl_2O_4$–TiO_2 (8 : 2)	2.21	55.8	55.2	2.88	0.52
SO_4^{2-}/$ZnAl_2O_4$–TiO_2 (6 : 4)	2.31	63.8	75.8	3.15	0.68
SO_4^{2-}/$ZnAl_2O_4$–TiO_2 (4 : 6)	1.62	40.2	52.6	2.83	0.67
SO_4^{2-}/$ZnAl_2O_4$–TiO_2 (2 : 8)	1.69	36.6	63.1	2.47	0.78
SO_4^{2-}/TiO_2	2.16	69.8	70.9	3.69	0.68

[a] TOF = M_{acid}/M_{site}, where M_{acid} and M_{site} are mole of the initial acid consumed in the reaction per unit time (min) and mole of active sites, respectively. M_{site} is obtained from the result of acid–base titration for each catalyst.

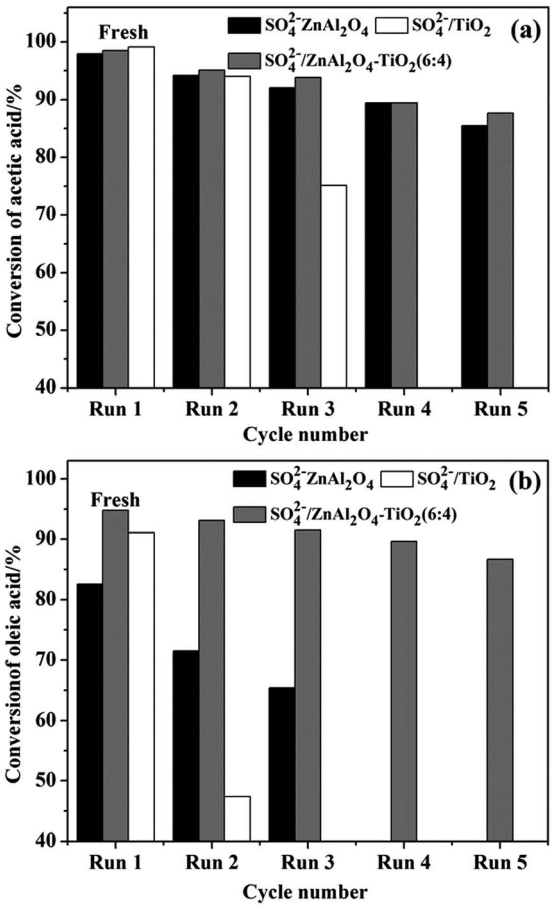

Fig. 10 Reusability of $SO_4^{2-}/ZnAl_2O_4$, SO_4^{2-}/TiO_2 and $SO_4^{2-}/ZnAl_2O_4$–TiO_2 (6 : 4) catalysts for esterification of (a) acetic acid with *n*-butanol and (b) oleic acid with methanol.

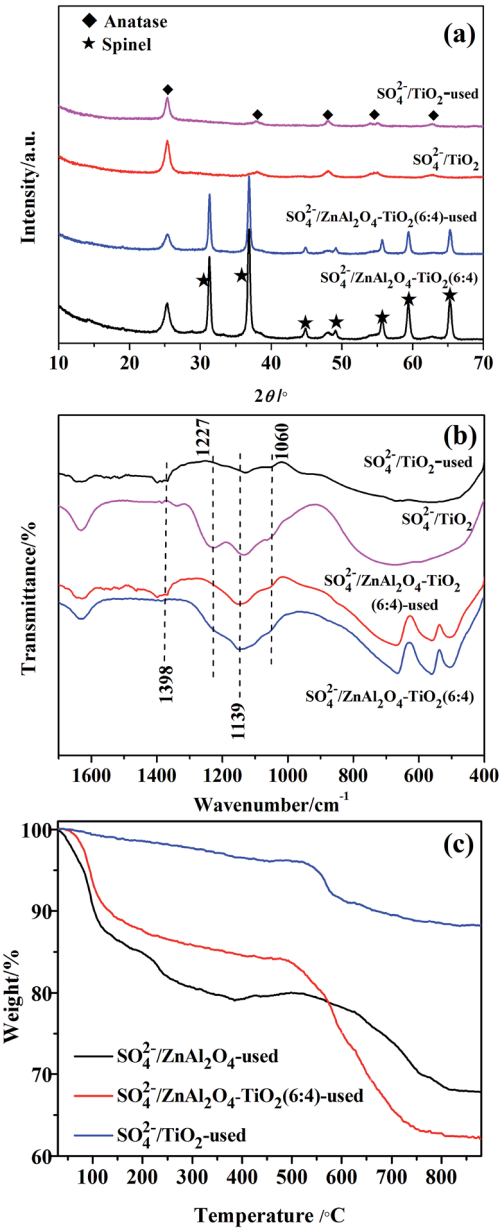

Fig. 11 XRD (a), FT-IR (b) and TG (c) patterns of fresh and used catalysts.

of used $SO_4^{2-}/ZnAl_2O_4$–TiO_2. $SO_4^{2-}/ZnAl_2O_4$–TiO_2 had superior resistance to the loss of sulfur species, which might interpret its better reusability. The TG curves in Fig. 11c were also performed to estimate the amount of residual sulfate groups on the surface of the used catalysts. As shown in Table 1, the weight percentages of surface sulfate groups on the used $SO_4^{2-}/ZnAl_2O_4$, $SO_4^{2-}/ZnAl_2O_4$–TiO_2 (6 : 4) and SO_4^{2-}/TiO_2 were estimated to be 10.9%, ~16.2% and ~7.8%, respectively. $ZnAl_2O_4$-based catalysts showed relatively minimal sulfur loss particularly in the $SO_4^{2-}/ZnAl_2O_4$–TiO_2 (6 : 4) catalysts. Accordingly, it was suggested that the $ZnAl_2O_4$ component played a significant role in stabilizing sulfate groups on the surface of the $SO_4^{2-}/ZnAl_2O_4$–TiO_2 catalyst and enhance its resistance of sulfur loss, which was also approved in IR analysis. Based on IR and TG analysis, a decrease in the intensity of peaks and the number of sulfate groups was observed in all used catalysts. This indicated that the catalysts inevitably suffered from the loss of sulfur species. The loss of surface sulfate groups is one of the main reasons for the deactivation of these catalysts in recycling reaction, which is common in other sulfated catalysts.[40–42]

Table 3 lists these two types of esterifications over various catalysts, such as modified SO_4^{2-}/TiO_2, MCM-41, MOFs, and H_2SO_4, and compares the reported catalysts with catalysts obtained in this study. The results showed that the high conversion in the esterification of acetic acid *n*-butanol over $SO_4^{2-}/ZnAl_2O_4$–TiO_2 (6 : 4) was comparable to that of modified SO_4^{2-}/TiO_2 and Al–MCM-41 mesoporous catalysts presented in the literature, whereas the relatively milder reaction condition was applied in this study.[9,43,44] For the esterification of oleic acid with methanol, the $SO_4^{2-}/ZnAl_2O_4$–TiO_2 (6 : 4) catalyst with a smaller catalyst amount and shorter reaction time exhibited a higher catalytic activity (95.8%) than [TMEDAPS][HSO_4] and MOF-808-2.5SO_4.[6,45] Although a homogeneous acid, *i.e.*, H_2SO_4, showed high conversion (91%) in low molar ratio of alcohol to acid and at low temperature,[46] the use of eco-friendly heterogeneous catalysts was more advantageous due to the easy separation and re-use of the catalyst. This suggested that the

Table 3 Comparison of catalytic activity of the $SO_4^{2-}/ZnAl_2O_4–TiO_2$ (6 : 4) catalyst with other reported solid acid catalysts

	Reaction conditions							
Catalyst	Amount[a]/wt%	Acid	Alcohol	Molar ratio[b]	Temp./°C	Time/h	Conv./%	Ref.
SO_4^{2-}/TiO_2–Zr–La	14.3	Acetic acid	*n*-Butanol	1.56 : 1	98–112	0.5	85	9
$SO_4^{2-}–Ce_{0.02}/TiO_2$	12	Acetic acid	*n*-Butanol	3/1	145	0.75	97.1	43
Al–MCM-41 (Si/Al = 25)	1.67	Acetic acid	*n*-Butanol	1/2	125	6	87.3	44
$SO_4^{2-}/ZnAl_2O_4–TiO_2$ (6 : 4)	7.3	Acetic acid	*n*-Butanol	3/1	115	2	98.5	—[c]
MOF-808-2.5SO_4	20	Oleic acid	Methanol	70/1	65	6	80	6
H_2SO_4	—	Oleic acid	Methanol	3/1	80	6	91	46
[TMEDAPS][HSO_4]	0.2 : 1.8[d]	Oleic acid	Methanol	1.8/1	70	6	95	45
$SO_4^{2-}/ZnAl_2O_4–TiO_2$ (6 : 4)	5	Oleic acid	Methanol	10/1	100	2	95.8	—[c]

[a] Based on the acid. [b] The molar ratio of acid to alcohol. [c] Present study. [d] *n*([TMEDAPS][HSO_4]) : *n*(Methanol).

$SO_4^{2-}/ZnAl_2O_4–TiO_2$ (6 : 4) is more or less superior compared to the reported catalysts in terms of the high acid conversion with short reaction times and mild conditions, easy recoverability and high recyclability.

4. Conclusions

This study synthesized a series of novel $SO_4^{2-}/ZnAl_2O_4–TiO_2$ composite catalysts with single spinel and anatase phases and applied these catalysts in the esterification of biomass derived acids. In the composite catalyst, both $ZnAl_2O_4$ and TiO_2 oxides acted as catalytic components, and generated acid sites by sulfation. The catalytic properties and performance of composite catalysts can be tuned by adjusting the mass ratio of $ZnAl_2O_4$/TiO_2. The optimal $SO_4^{2-}/ZnAl_2O_4–TiO_2$ (6 : 4) exhibited excellent conversion of 95.8% and 98.5% in oleic acid and acetic acid esterification, respectively, which was attributed to the larger number of acid sites due to the cooperation of $ZnAl_2O_4$ and TiO_2 oxides. In addition, the $ZnAl_2O_4$ component played a key role in stabilizing the structural stability as well as the surface sulfate groups. The advantage of superior reusability accordingly showed in the $SO_4^{2-}/ZnAl_2O_4–TiO_2$ (6 : 4) catalyst with high conversion above 85% up to 5 cycles for both esterification reactions. Correlating the acidic properties and activities, it was assumed that the amount of acid sites varied in acid strength on the different catalysts so that these catalysts performed differently for these two reactions. The esterification of acetic acid and *n*-butanol may require strong acid sites, while middle strength or weak acid sites were favorable to the esterification of oleic acid with methanol.

This study suggested that the $ZnAl_2O_4$ spinel oxide can be used as a novel component to modify the SO_4^{2-}/M_xO_y catalyst. The spinel-type component in composites plays a role in tuning the catalytic properties and stabilizing the structure and surface sulfate groups.

Acknowledgements

This study has been financially supported by the National Natural Science Foundation of China (NSFC No. 21203170) and the National College Students' Innovative Training Program (NCSITP No. 201610491017 and 201610491033).

Notes and references

1 P. A. Alaba, Y. M. Sanib and W. M. A. W. Daud, *RSC Adv.*, 2016, **6**, 78351–78368.
2 J. A. Melero, J. Iglesias and G. Morales, *Green Chem.*, 2009, **54**, 1285–1308.
3 A. F. Lee, J. A. Bennett, J. C. Manayil and K. Wilson, *Chem. Soc. Rev.*, 2014, **43**, 7887–7916.
4 K. Saravanan, B. Tyagi, R. S. Shukla and H. C. Bajaj, *Fuel*, 2016, **165**, 298–305.
5 L. S. Do Nascimento, L. M. Z. Tito, R. S. Angélica, C. E. F. Da Costa, J. R. Zamian and G. N. Da Rocha Filho, *Appl. Catal., B*, 2011, **101**, 495–503.
6 J. Jiang, F. Gándara, Y. B. Zhang, K. Na, O. M. Yaghi and W. G. Klemperer, *J. Am. Chem. Soc.*, 2014, **136**, 12844–12847.
7 K. Arata, *Adv. Catal.*, 1990, **37**, 165–211.
8 Y. Li, X. D. Zhang, L. Sun, J. Zhang and H. P. Xu, *Appl. Energy*, 2010, **87**, 156–159.
9 W. P. Shi, *Catal. Lett.*, 2010, **143**, 732–738.
10 M. Yang, Y. Men, S. L. Li and G. W. Chen, *Appl. Catal., A*, 2012, **433–434**, 26–34.
11 Q. Lu, X. N. Ye, Z. B. Zhang, C. Q. Dong and Y. Zhang, *Bioresour. Technol.*, 2014, **171**, 10–15.
12 A. Q. Wang, X. L. Wu, J. X. Wang, H. Pan, X. Y. Tian and Y. L. Xing, *RSC Adv.*, 2015, **5**, 19652–19658.
13 J. X. Wang, A. Q. Wang, Y. L. Xing, Z. X. Zhu, X. L. Wu, Y. Q. Wang and L. X. Yang, *RSC Adv.*, 2015, **5**, 105908–105916.
14 J. X. Wang, H. Pan, A. Q. Wang, X. Y. Tian, X. L. Wu and Y. Q. Wang, *Catal. Commun.*, 2015, **62**, 29–33.
15 K. R. Sunajadevi and S. Sugunan, *Catal. Commun.*, 2004, **5**, 575–581.
16 C. Morterra, G. Cerrato, F. Pinna and M. Signoretto, *J. Catal.*, 1995, **157**, 109–123.
17 A. Patel and N. Narkhede, *Energy Fuels*, 2012, **26**, 6025–6032.
18 G. Corro, F. Bañuelos, E. Vidal and S. Cebada, *Fuel*, 2014, **115**, 625–628.
19 J. C. Manayil, C. V. M. Inocencio, A. F. Lee and K. Wilson, *Green Chem.*, 2016, **18**, 1387–1394.
20 R. Hilten, J. Weber and J. R. Kastner, *Energy Fuels*, 2016, **30**, 9480–9489.

21 E. Tabrizian and A. Amoozadeh, *RSC Adv.*, 2016, **6**, 96606–96615.
22 Y. Wang, D. Wang, M. H. Tan, B. Jiang, J. T. Zheng, N. Tsubaki and M. B. Wu, *ACS Appl. Mater. Interfaces*, 2015, **7**, 26767–26775.
23 L. H. O. Pires, A. N. De Oliveira, O. V. Monteiro Jr, R. S. Angélica, C. E. F. Da Costa, J. R. Zamian, L. A. S. Do Nascimento and G. N. Rocha Filho, *Appl. Catal., B*, 2014, **160–161**, 122–128.
24 G. D. Yadav and R. V. Sharma, *J. Catal.*, 2014, **311**, 121–128.
25 C. C. Huang, C. J. Yang, P. J. Gao, N. C. Wang, C. L. Chen and J. S. Chang, *Green Chem.*, 2015, **17**, 3609–3620.
26 F. Haase and J. Sauer, *J. Am. Chem. Soc.*, 1998, **120**, 13503–13512.
27 Z. L. Li, R. Wnetrzak, W. Kwapinski and J. J. Leahy, *ACS Appl. Mater. Interfaces*, 2012, **4**, 4499–4505.
28 K. Saravanan, B. Tyagi, R. S. Shukla and H. C. Bajaj, *Appl. Catal., B*, 2015, **172–173**, 108–115.
29 S. Farhadi and S. Panahandehjoo, *Appl. Catal., A*, 2010, **382**, 293–302.
30 D. Ma, Y. J. Xin, M. C. Gao and J. Wu, *Appl. Catal., B*, 2014, **147**, 49–57.
31 H. Y. Zhao, S. Bennici, J. Y. Shen and A. Auroux, *J. Catal.*, 2010, **272**, 176–189.
32 L. J. Liu, G. L. Zhang, L. Wang, T. Huang and L. Qin, *Ind. Eng. Chem. Res.*, 2011, **50**, 7219–7227.
33 X. L. Duan, D. R. Yuan and F. P. Yu, *Inorg. Chem.*, 2011, **50**, 5460–5467.
34 L. C. Peng, L. Lin, H. Li and Q. L. Yang, *Appl. Energy*, 2011, **88**, 4590–4596.
35 B. M. Reddy, B. Chowdhury and P. G. Smirniotis, *Appl. Catal., A*, 2001, **211**, 19–30.
36 M. E. Manríquez, T. López, R. Gómez and J. Navarrete, *J. Mol. Catal. A: Chem.*, 2004, **220**, 229–237.
37 T. Wu, J. W. Wan and X. B. Ma, *Chin. J. Catal.*, 2015, **36**, 425–431.
38 T. Witoon, T. Permsirivanich, N. Kanjanasoontorn, C. Akkaraphataworn, A. Seubsai, K. Faungnawakij, C. Warakulwit, M. Chareonpanich and J. Limtrakul, *Catal. Sci. Technol.*, 2015, **5**, 2347–2357.
39 K. Ngaosuwan, J. G. Goodwin Jr and P. Prasertdham, *Renewable Energy*, 2016, **86**, 262–269.
40 J. Zhu, P. C. Wang and M. Lu, *Catal. Sci. Technol.*, 2015, **5**, 3383–3393.
41 L. Zhang, W. X. Zou, K. L. Ma, Y. Cao, Y. Xiong, S. G. Wu, C. J. Tang, F. Gao and L. Dong, *J. Phys. Chem. C*, 2014, **119**, 1155–1163.
42 K. Suwannakarn, E. Lotero, J. G. Goodwin Jr and C. Q. Lu, *J. Catal.*, 2008, **255**, 279–286.
43 G. Xiao, J. F. Zhou, X. Huang, X. P. Liao and B. Shi, *RSC Adv.*, 2014, **4**, 4010–4019.
44 B. R. Jermy and A. Pandurangan, *Appl. Catal., A*, 2005, **288**, 25–33.
45 D. Fang, J. M. Yang and C. M. Jiao, *ACS Catal.*, 2011, **1**, 42–47.
46 J. Y. Park, Z. M. Wang, D. K. Kim and J. S. Lee, *Renewable Energy*, 2010, **35**, 614–618.

